

## TMD gluon density determination from combined DIS data

---

**Hannes JUNG\***

*DESY, Hamburg, FRG*

*University of Antwerp, Antwerp, Belgium*

*E-mail: [hannes.jung@desy.ch](mailto:hannes.jung@desy.ch)*

**Francesco HAUTMANN**

*Dept. of Physics and Astronomy, University of Sussex, Brighton BN1 9QH*

*Rutherford Appleton Laboratory, Chilton OX11 0QX*

*Dept. of Theoretical Physics, University of Oxford, Oxford OX1 3NP*

*E-mail: [hautmann@thphys.ox.ac.uk](mailto:hautmann@thphys.ox.ac.uk)*

We report on fits to deep inelastic scattering (DIS) data using transverse momentum dependent QCD factorization and CCFM evolution. The results of the fits to precision DIS measurements are used to make a determination of the non-perturbative transverse momentum dependent gluon density function, including experimental and theoretical uncertainties.

*XXII. International Workshop on Deep-Inelastic Scattering and Related Subjects*

*28 April - 2 May 2014*

*Warsaw, Poland*

---

\*Speaker.

## 1. Introduction

In this paper, based on [1], combined data on inclusive deep-inelastic scattering [2] and deep-inelastic charm production [3] are used for determination of transverse-momentum dependent (TMD), or unintegrated, parton densities. We limit ourselves to DIS in the small- $x$  kinematic region, where a well-defined form of TMD factorization holds at high energy [4]. This high-energy factorization expresses the heavy-quark lepto-production cross section in terms of the TMD gluon density and calculable perturbative matrix elements. This framework is extended to inclusive DIS in [5]. Phenomenological applications of this approach require matching of small- $x$  contributions with contributions from medium and large  $x$  [6–12]. We have developed further the parton branching Monte Carlo [11] implementation of the CCFM evolution equation [13–15], which we include in the `herafitter` program [2, 16]. The TMD gluon distribution at the initial scale  $q_0$  of the evolution is determined from fits to DIS data, including charm production.

We perform fits to measurements of inclusive DIS [2] in the range  $x < 0.005$ ,  $Q^2 > 5 \text{ GeV}^2$  and to measurements of deep-inelastic charm production [3] in the range  $Q^2 > 2.5 \text{ GeV}^2$ . We obtain good fits, and we determine the TMD gluon density. We find that the best fit to DIS charm gives  $\chi^2$  per degree of freedom  $\chi^2/ndf \simeq 0.63$ , and the best fit to inclusive DIS gives  $\chi^2/ndf \simeq 1.18$ . We also determine experimental and theoretical uncertainties of the TMD gluon.

## 2. Cross section calculation and evolution of TMD gluon density at small $x$

In the framework of high-energy factorization [4] the deep-inelastic scattering cross section is written as a convolution in both longitudinal and transverse momenta of the TMD parton density function  $\mathcal{A}(x, k_t, \mu)$  with off-shell partonic matrix elements, as follows

$$\sigma_j(x, Q^2) = \int_x^1 dz \int d^2k_t \hat{\sigma}_j(x, Q^2, z, k_t) \mathcal{A}(z, k_t, \mu). \quad (2.1)$$

Here  $x$  and  $Q^2$  denote the Bjorken variable and photon virtuality, and the DIS cross sections is given by  $\sigma_j$ , with  $j = 2, L$ . The calculation of the cross section according to Eq. (2.1) involves a multidimensional Monte Carlo integration which is time consuming and suffers from numerical fluctuations. This cannot be employed directly in a fit procedure involving the calculation of numerical derivatives in the search for the minimum. Instead the following procedure [17] is applied:

$$\begin{aligned} \sigma(x, Q^2) &= \int_x^1 dx_g \mathcal{A}(x_g, k_t, p) \hat{\sigma}(x, x_g, Q^2) \\ &= \int dx_g dx' dx'' \mathcal{A}_0(x') \tilde{\mathcal{A}}(x'', k_t, p) \cdot \hat{\sigma}(x, x_g, Q^2) \cdot \delta(x' x'' - x_g) \\ &= \int_x^1 dx' \mathcal{A}_0(x') \cdot \int_{x/x'}^1 dx'' \tilde{\mathcal{A}}(x'', k_t, p) \cdot \hat{\sigma}(x, x' x'', Q^2) \\ &= \int_x^1 dx' \mathcal{A}_0(x') \cdot \tilde{\sigma}(x/x', Q^2) \end{aligned} \quad (2.2)$$

Here, first  $\tilde{\sigma}(x', Q^2)$  is calculated numerically with a Monte Carlo integration on a grid in  $x$  for the values of  $Q^2$  used in the fit. Then the last step in Eq.(2.2) is performed using a fast numerical gauss integration, which can be used in standard fit procedures.

The fit to the HERA DIS measurements is performed by applying the `herafitter` package [2, 16] to determine the parameters of the starting distribution  $\mathcal{A}_0$  at the starting scale  $q_0$ . We perform fits by using the three-parameter form

$$x\mathcal{A}_0(x, k_t) = Nx^{-B} \cdot (1-x)^C \exp[-k_t^2/\sigma^2] . \quad (2.3)$$

We take  $\sigma^2 = q_0^2/2$ . The parameters  $N, B, C$ , in Eq. (2.3) are determined by fitting the high-precision inclusive DIS measurements [2] in the range  $x < 0.005$  and  $Q^2 > 5 \text{ GeV}^2$ , and charm production measurements [3] in the range  $Q^2 > 2.5 \text{ GeV}^2$ . The results are obtained with the `herafitter` package by treating the correlated systematic uncertainties separately from the uncorrelated statistical and systematic uncertainties.

We include two-loop running coupling, gluon splitting and consistency constraint and, in addition to the gluon-induced process  $\gamma^* g^* \rightarrow q\bar{q}$ , the contribution from valence quarks is included via  $\gamma^* q \rightarrow q$  by using a CCFM evolution of valence quarks [18]. Fig. 1 shows the description of the inclusive DIS cross section [2], by the individual fits and a combined fit. Plotted are the reduced cross sections defined in [2, 3].

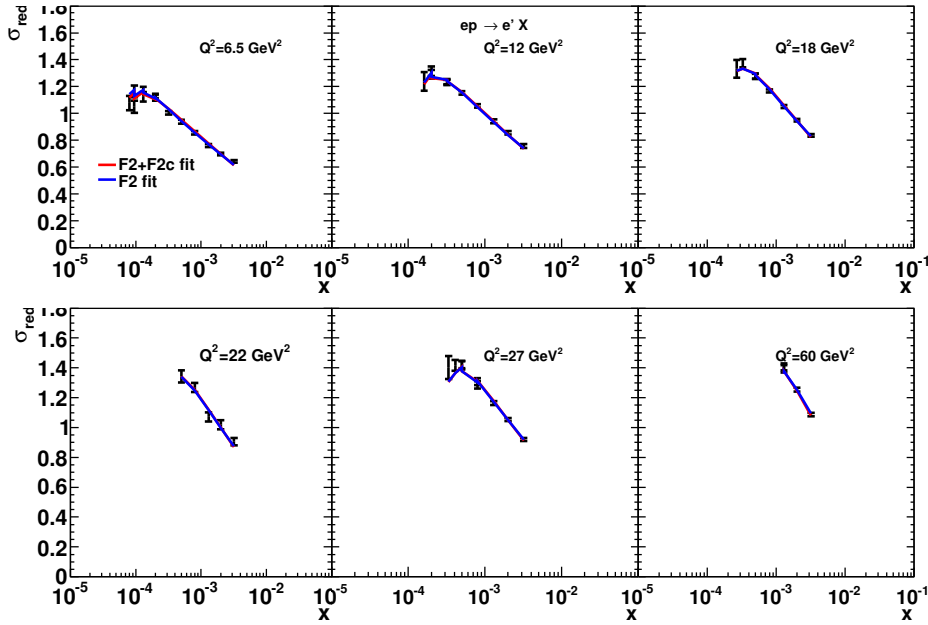


**Figure 1:** The fit to DIS high-precision data: (top) charm lepto-production data [3]; (bottom) inclusive structure function data [2].

We present two sets of unintegrated pdfs determined from the fits to high-precision DIS measurements: JH-2013-set1 is determined from the fit to inclusive DIS data only; JH-2013-set2 is determined from the fit to both inclusive DIS and charm data. The unintegrated TMD gluon density is shown in Figs. 2, versus the longitudinal momentum fraction  $x$  and versus the transverse momentum  $k_t$ . The results are compared with the older parton distribution set A0 [19], which did not use the precision data and did not include two-loop running coupling, kinematic consis-

tency constraint, nonsingular terms in the gluon splitting function, and unintegrated valence quark density.

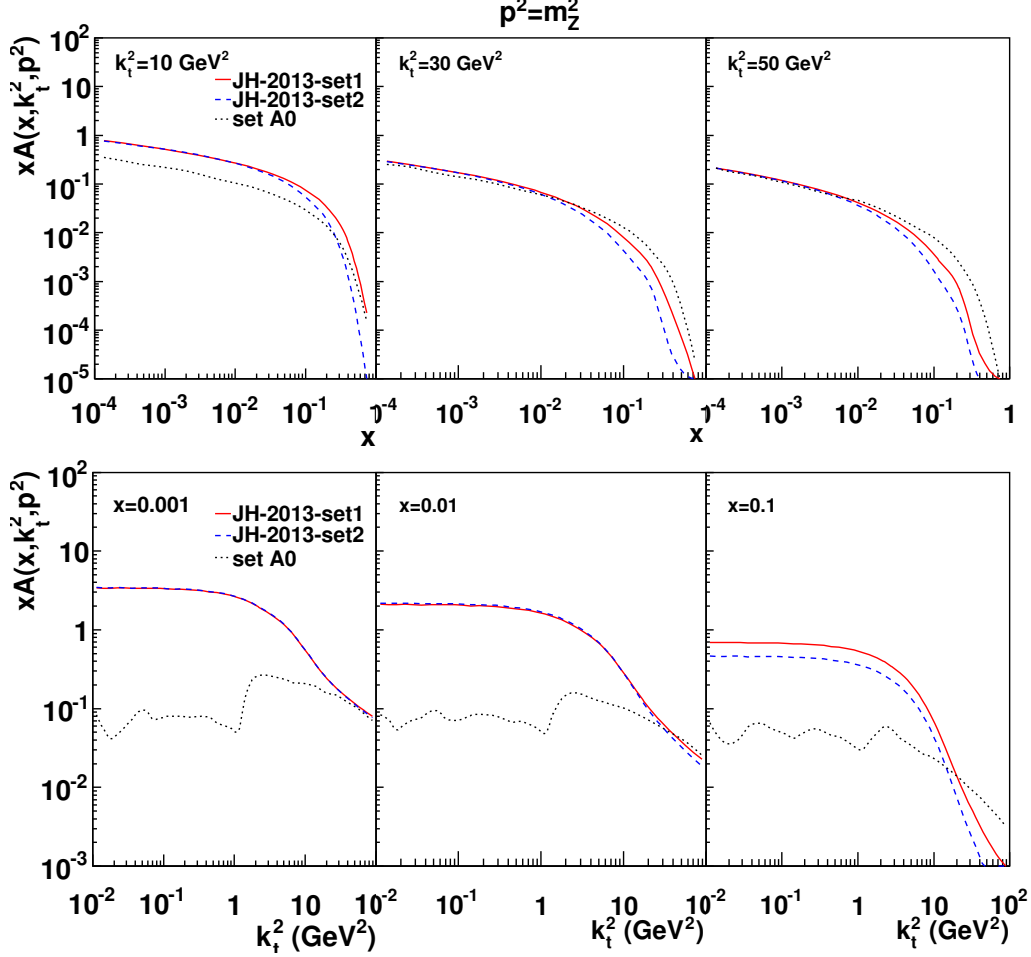


**Figure 2:** Unintegrated TMD gluon density (JH-2013-set1 and JH-2013-set2) at evolution scale equal to the Z-boson mass,  $p^2 = m_Z^2$ : (top) as a function of  $x$  for different values of  $k_t^2$ ; (bottom) as a function of  $k_t^2$  for different values of  $x$ . The results are compared with set A0 [19].

We also consider theoretical uncertainties. The first such kind of uncertainty is the dependence on the starting scale  $q_0$  for gluon density evolution. In Figs. 3 the dotted blue curves show the effect on the gluon distribution from variation in the starting scale  $q_0$ . These uncertainties are small at small  $x$ , while they become very large at large  $x$  because in this region, since we fit DIS in the range  $x < 0.005$  and  $Q^2 > 5$  GeV<sup>2</sup>, there is little constraint from data.

We also consider theoretical uncertainties on the TMD gluon density from variation of the factorization scale and renormalization scale. This approach is different from that usually followed in determinations of ordinary, collinear pdfs from fixed-order perturbative treatments [20]. In this case, no uncertainty on the pdfs is considered from scale variation. Only when computing predictions for any specific observable the theoretical uncertainty on the predictions is estimated by scale

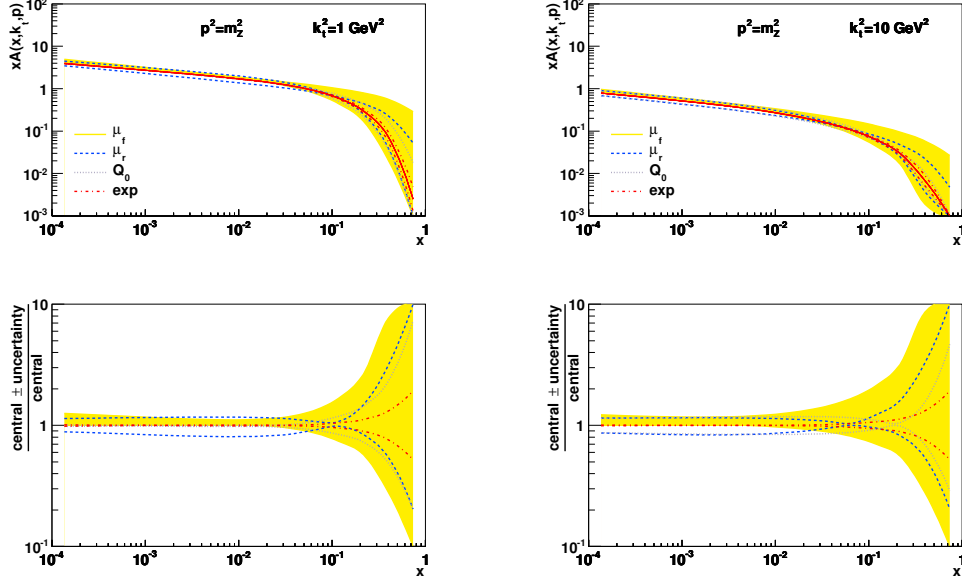


**Figure 3:** Experimental and theoretical uncertainties of the unintegrated TMD gluon density versus  $x$  for different values of transverse momentum at  $p^2 = m_Z^2$ . The yellow band gives the uncertainty from the factorization scale variation; the curves indicate the uncertainties from the other sources.

variation. In our approach we are interested to estimate the uncertainty from varying scales in the theoretical calculation used to determine the pdf. In Figs. 3 the renormalization scale (blue dashed curves) and in the factorization scale (yellow band) are varied by a factor of 2.

An application of the newly determined TMD gluon and valence quark densities is reported in [21] for  $W + jet$  production in  $pp$  at LHC energies. A very good description of the measurements of ATLAS and CMS is obtained even for high  $p_t$  multi-jet distributions.

### 3. Summary

A first determination of the TMD gluon density function from high-precision DIS measurements, including experimental and theoretical uncertainties, has been performed. We fit the combined HERA data and find a good fit to both charm-quark and inclusive measurements. We determine the TMD gluon density and present new unintegrated pdf sets, JH-2013. As a result of the high-precision data, the JH-2013 distributions differ significantly from earlier sets. We also present separate results for the different contributions to the experimental and theoretical uncertainties associated with the TMD pdfs.

### Acknowledgements

We are grateful to the organisers of DIS and the conveners and participants of the working group on structure functions for productive discussions.

## References

- [1] F. Hautmann and H. Jung, Nucl. Phys. **B883** (2014) 1.
- [2] F. Aaron *et al.*, JHEP **1001** (2010) 109.
- [3] H. Abramowicz *et al.*, Eur. Phys. J. C **73** (2013) 2311.
- [4] S. Catani, M. Ciafaloni and F. Hautmann, Phys. Lett. **B307** (1993) 147; Nucl. Phys. **B366** (1991) 135; Phys. Lett. **B242** (1990) 97.
- [5] S. Catani and F. Hautmann, Nucl. Phys. **B427** (1994) 475; Phys. Lett. **B315** (1993) 157.
- [6] G. Altarelli, R. Ball and S. Forte, Nucl. Phys. **B799** (2008) 199; M. Ciafaloni, D. Colferai, G.P. Salam and A. Stasto, JHEP **0708** (2007) 046; R.S. Thorne, Phys. Rev. **D60** (1999) 054031; R.K. Ellis, F. Hautmann and B.R. Webber, Phys. Lett. **B** 348 (1995) 582.
- [7] B. Andersson *et al.* Eur. Phys. J. **C25** (2002) 771, [arXiv:hep-ph/0204115](#).
- [8] H. Jung, Mod. Phys. Lett. **A19** (2004) 1.
- [9] F. Hautmann and H. Jung, JHEP **0810** (2008) 113; [arXiv:0804.1746](#) [hep-ph].
- [10] Z. Ajaltouni *et al.*, [arXiv:0903.3861](#) [hep-ph].
- [11] G. Marchesini and B.R. Webber, Nucl. Phys. **B386** (1992) 215; Nucl. Phys. **B349** (1991) 617.
- [12] S. Catani, M. Ciafaloni and F. Hautmann, in Proc. HERA Workshop, eds. W. Buchmüller and G. Ingelman (Hamburg 1992), p. 690; Nucl. Phys. B Proc. Suppl. **29A** (1992) 182.
- [13] M. Ciafaloni, Nucl. Phys. **B296** (1988) 49.
- [14] S. Catani, F. Fiorani and G. Marchesini, Nucl. Phys. **B336** (1990) 18; G. Marchesini, Nucl. Phys. **B445** (1995) 49.
- [15] F. Hautmann, H. Jung, S. Taheri-Monfared, DESY 14-060.
- [16] “HERAFitter” (2012), ; F. Aaron *et al.* Eur. Phys. J. **C64** (2009) 561, [arXiv:0904.3513](#) [hep-ex]; F. James and M. Roos, Comput. Phys. Commun. **10** (1975) 343.
- [17] F. Hautmann and H. Jung, PoS DIS2013 (2013) 053; [arXiv:1206.1796](#) [hep-ph].
- [18] M. Deak, F. Hautmann, H. Jung and K. Kutak, [arXiv:1012.6037](#) [hep-ph]; Eur. Phys. J. C **72** (2012) 1982.
- [19] H. Jung *et al.*, Eur. Phys. J. C **70** (2010) 1237.
- [20] S. Alekhin *et al.*, [arXiv:1101.0536](#) [hep-ph].
- [21] S. Dooling, F. Hautmann, and H. Jung, [arXiv:1406.2994](#) [hep-ph].